Electric Vehicle Mobility in Transmission-Constrained Hourly Power Generation Scheduling

Mohammad E. Khodayar, *Member, IEEE*, Lei Wu, *Member, IEEE*, and Zuyi Li, *Senior Member, IEEE*

***Abstract*—The proposed approach evaluates the effect of integrating a large number of electric vehicles (EVs) on power grid operation and control. The EV fleets could serve as electricity load when drawing energy from the grid and as energy storage (vehicle-to-grid) when delivering energy to the grid. The paper considers two operating modes for EV fleets which are consumer-controlled and grid-controlled. The power grid generation mix represents a multitude of units including thermal, hydro, and wind. The paper considers the impact of EV battery utilization on offsetting the hourly variability of wind generation units in transmission-constrained power grids. The paper considers charging/discharging schedule of EV batteries and consumer driving requirements on the optimal hourly transmission-constrained commitment and dispatch of generation units in the day-ahead scheduling. The hourly solution of the proposed method will minimize the cost of supplying the hourly load while satisfying the temporal constraints of individual components in power grids.**

***Index Terms*—Day-ahead scheduling, EV mobility, variability of wind energy, vehicle-to-grid (V2G).**

NOMENCLATURE

Variables

b, j, o	Indexes of bus.
$C_{(.)}$	Operation cost of EV fleet.
$E_{v,t}$	Available energy in batteries of fleet v at time t.
$E^{net}_{v,t}$	Net discharged energy of EV fleet v at time t.
$F_{c,i}$	Production cost function of a thermal unit i.
i	Denote a thermal unit.
$I_{(.)}$	Unit status indicator, 1 means on and 0 means off.
$I_{c,(.)}$	Indicator of an EV fleet in charging mode.
$I_{dc,(.)}$	Indicator of an EV fleet in discharging mode.
$I_{i,(.)}$	Indicator of an EV fleet in idle mode.
k	Denote a hydro unit.
l	Index of transmission line.
m	Denote a segment of curves.
$MP_{(.),t,b}$	Non-negative slack variables for real power mismatch at bus b at hour t.
$P_{(.)}$	Generation of a unit.
$P_{d,w,t}$	Curtailment of wind unit w at hour t.
$P_{c,(.)}, P_{dc,(.)}$	Charging/discharging power of an EV fleet.
$P_{m,(.)}$	Charging/discharging power rate at segment m.
$PL_{l,t}$	Real power flow on line l at hour t.
$q_{(.)}$	Water discharge rate.
$q_{m,(.)}$	Water discharge rate at segment m of a unit.
$SD_{(.)}$	Shutdown cost of a unit.
$SU_{(.)}$	Startup cost of a unit.
t	Hour index.
v	Denote an EV fleet.
w	Denote a wind unit.
$W_{(.)}$	Objective function value of a subproblem.
$\theta_{(.)}$	Bus angle.
λ, π, ρ, μ	Lagrangian multipliers.
$\delta^m_{k,(\cdot)}$	Binary variable for water-to-power curve.

Constants:

$B^{(.)}_{b,t}$	Set of units which are connected to bus b at time t.
$b_{m,(.)}$	Slope of segment m in linearized generation curve.
CD_k, CS_k	Shutdown/startup cost of hydro unit k.
D_b	Set of loads which are connected to bus b.
$E^{\min}_v, E^{\max}_v$	Min/max energy stored in batteries of EV fleet v.
$L_{f,b}, L_{t,b}$	Set of transmission lines starting from/ending at bus b.
$N_{v,t}$	Binary parameter indicating the grid connection status of fleet v at time t.
$NM_{(.)}$	Number of segments in water-to-power conversion curve
NT	Number of hours under study.

Manuscript received October 24, 2012; revised nulldate; accepted November 17, 2012. This project is supported in part by the U.S. Department of Energy under Grants DE-EE 0002979 and DE-EE 0001380.000. Paper no. TSG-00754-2012.

M. E. Khodayar and Z. Li are with Electrical and Computer Engineering Department, Illinois Institute of Technology, Chicago, IL 60616 USA (e-mail: mkhodaya@iit.edu; lizu@iit.edu).

L. Wu is with Electrical and Computer Engineering Department, Clarkson University, Potsdam, NY 13699 USA (e-mail: lwu@clarkson.edu).

Color versions of one or more of the figures in this paper are available online at http://ieeexplore.ieee.org.

Digital Object Identifier 10.1109/TSG.2012.2230345

$P_{(.)}^{min}, P_{(.)}^{max}$	Min/max generation capacity.
$P_{c,v}^{\min}, P_{c,v}^{\max}$	Min/max charging capacity of EV fleet v.
$P_{dc,v}^{\min}, P_{dc,v}^{\max}$	Min/max discharging capacity of EV fleet v.
$P_{D,(.)}$	Total demand in power grid
$P_{f,w,t}$	Wind power forecast of unit w at hour t.
$P_{m,v}^{\max}$	Max power output at segment m in charging/discharging cost curve of EV fleet v.
$PL_l^{\max}$	Max capacity of line l.
$q_{(\cdot)}^{\min}$	Min water discharge of a unit in generation mode.
$q_{m,(\cdot)}^{\max}$	Max water discharge at segment m in water to power conversion curve.
$\hat{T}$	Time in which the state of charge is set to specific value during the operation period.
X_{jo}	Inductance of a line between buses j and o.
η_v	Efficiency of charging cycle of EV fleet.

I. Introduction

THE transportation industry holds approximately one third of the total share of the greenhouse gas (GHG) production in the United States [1]. Environmental concerns over the GHG production and the adverse economic effects of dependency on fossil fuel imports are expected to have a major impact on the EV utilization in many countries. The Energy Technology Perspective (ETP) 2010 sets a 50% reduction in the global CO_2 emission by 2050 as compared to 2005 in which the contribution of the transportation sector would reduce the CO_2 emission to 30% below that of 2005. This is achieved by the annual sale of a few million EVs and PHEVs in which EV sales represents a 50% of the total sales [2]. As the EV penetration level increases in power systems, the storage capacity provided by EV would be prominent. Aggregated EVs can act as distributed and mobile demand and storage (V2G) which can decrease the operation cost of power grids. The resulting bi-directional power flow would reduce the impact of uncertainties imposed on power grids by the high penetration of renewable energy resources [3]–[6].

The EV mobility would also affect potential costs/revenues in regional electricity markets. V2G technology is currently at its early stages of conceptual planning which can adopt remotely controlled bi-directional energy flows. The V2G implementation would require prevalent adoption of smart charging stations, additional upgrades in energy and communication infrastructure, more utility standards, and EVs equipped with V2G-enabled communication hardware/software. Additional standards, guidelines and practices are required to facilitate the widespread integration of V2G technology in power systems. This includes the development of IEEE 1547.3 which provides guidelines for the monitoring, information exchange and the control of distributed resources in electric power systems. Moreover SAE J1772 (conductive charge coupler for PHEV and EV) and SAE J2293 (energy transfer system for EV) along with IEEE 1547.3 are to be revised to address practical regulations on adoption of V2G technology.

There have been several studies on the integration of PHEVs into power systems. References [7], [8] evaluate the impact of coordinated charging of PHEVs on the voltage profile and network losses in distribution systems. In [9] the impact of PHEVs on reducing the transmission congestion through smart charging management schemes in energy hubs is evaluated. In [10] the effect of optimal dispatch of PHEV charging load on the system operating cost is evaluated. It is shown that incorporating the aggregated demand response programs would further optimize the power system operation. In [7]–[10], PHEVs are considered as the system demand in which V2G is not addressed, and the optimal charging sequence is determined according to several criteria. The modeling of PHEV is different than that of EV as there are resources other than the charging from the grid which are available to PHEV. Moreover, the battery capacity of a PHEV is usually smaller as the vehicle is equipped with internal combustion engine. Our proposed model with some minor modifications could be applied to the PHEV fleets.

Several studies have also covered the economic aspects of integrating EVs into electricity markets; however, they often lacked topological transmission constraints [11]. The stochastic modeling of aggregated EVs and their impact on the optimal load profile of power system is presented in [12].

This paper discusses the integration of aggregated EV fleets into constrained power systems and the potential benefits of V2G and mobility in the day-ahead generation scheduling of power systems. The effect of aggregated EV fleets on the optimal operation of power systems is investigated through several potential scenarios. V2G, mobility and consumer behaviors and their respective impacts on the optimal operation of power systems are addressed.

Considering the aggregators as the linkage between the distribution grid and the bus-level transmission grid, the EV optimization would be a two-stage solution:

1) The distribution level solution in which the aggregator would track the mobility of individual EVs and coordinate the EV charging sequence at the sub-transmission and distribution levels. The aggregator would provide the optimized plan, which is aggregated at the bus-level, to the ISO for the optimization of the day-ahead scheduling at the transmission level.
2) The ISO will execute the network-constrained unit commitment to procure the optimal generation schedule considering the generation and transmission constraints. The ISO would optimally dispatch the generation resources and send the corresponding scheduling signals back to the aggregators which would control the charging/discharging sequences of individual EVs considering the consumer's energy requirements in the day-ahead electricity market.

The iteration between the two stages would continue until an equilibrium point is procured. This paper addressed the second stage of the day-scheduling at the ISO level in which the aggregated EV fleets are represented in the day-ahead scheduling.

Fig. 1 shows the details of the information and control infrastructure in the proposed approach which facilitates the bi-directional information flow between individual EVs, distributed generation and load, aggregators, and the ISO. The advanced metering infrastructure (AMI) would facilitate the bi-directional communication and control signal flows from EV customers to

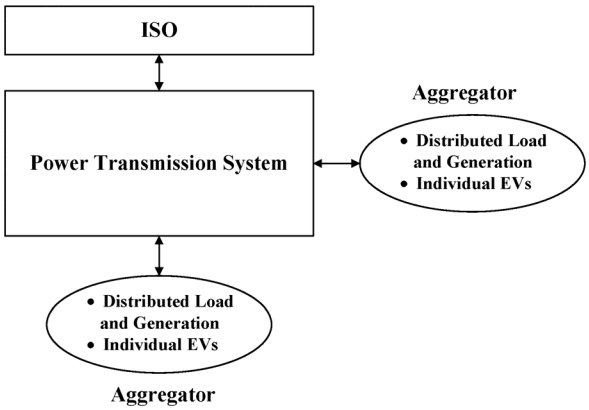

Fig. 1. Information exchange and control model for the integration of EV fleets.

aggregators. The process would include the required energy, battery state of charge and capacity, as well as the origin and the destination and travel times. The bi-directional mechanism can be implemented by connecting a device to each EV in a fleet which communicates with the aggregator through AMI. The communication hardware would be an extension to the EV charging station which enables the aggregator and consumers to monitor and control the charging/discharging sequences [13].

The aggregated EVs in this study are categorized based on their common driving patterns, including the points of origin and destination as well as the departure and arrival times. Hence the number of EVs with the same driving pattern at the aggregated level is large in the transmission system. The number of EVs in each fleet and their respective properties will determine the hourly state of charge (SOC), energy consumption, and max/min energy capacity supplied by the fleet of EVs. SOC is calculated as the ratio of the available energy in an EV battery to the maximum capacity of the battery. The driving energy consumption can be determined by the number of EVs in each fleet and their individual driving energy consumption.

We assume that the tracking of individual EVs would require the modeling of the low voltage and the medium voltage grids in the hourly SCUC for the day-ahead scheduling. The amount of data required for tracking individual EV units would be tremendously large for the purpose of the day-ahead scheduling. The aggregators will procure the total energy generation/consumption of EVs, storage capacity, and the marginal cost of charging/discharging through AMI for the participation in the day-ahead energy market.

The ISO level uncertainty corresponding to the wind speed, hourly demand, number of EV in each fleet, traveling times, driving patterns and their respective energy consumption would be considered in the Monte Carlo scenarios. The deterministic formulation in this paper could represent the EV fleets in each scenario [14]. The stochastic solution would procure the optimal day-ahead generation scheduling of power systems considering the uncertainties. Here, the expected system operation cost, because of the imposed uncertainties, would be higher than that of a deterministic solution.

Consumers can also impose further constraints on charging/discharging patterns of EVs. For instance, the consumers may fix the SOC of an EV at specific hours which will impose further restrictions on the optimal hourly scheduling problem.

In this paper, SOC is set at the specific user-defined value, i.e., 100%, before consumers leave a bus and drive to the next bus. The proposed formulation is an optimization problem which calculates the hourly network-constrained unit commitment and dispatch of generating units as well as the hourly charging/discharging schedule of EV fleets, considering the energy requirement and driving pattern of EVs, and other power grid constraints. The generation mix in the power grid would include variable wind generation units as well as thermal and hydro units. The hourly operation of entire set of generators will be coordinated with consumer-constrained EV fleet operations for minimizing the hourly cost of power generation scheduling. The wind speed variation is represented by the Weibull distribution function, the auto correlation factor, and the diurnal pattern [15]. The hourly wind generation is procured by utilizing the wind turbine power curve and wind speed data at wind power generation sites.

The rest of the paper is as follows. Section II discusses the proposed methodology. Section III illustrates the proposed methodology by a 6-bus and the IEEE 118-bus systems. Discussions and conclusions are presented in Sections IV and V, respectively.

II. Proposed Day-Ahead EV Scheduling Algorithm

The proposed network-constrained unit commitment is a mixed-integer programming (MIP) optimization problem. The network-constrained unit commitment is executed by the ISO for minimizing the cost of supplying the day-ahead load and to procure the optimal generation schedule considering the generation and transmission component constraints. The ISO optimally dispatches the generation resources available in the system and send signals to the aggregators to control the charging/discharging sequences of EV fleets considering the consumer's energy requirements in the day-ahead electricity market. At the distribution level, individual aggregators would maximize revenues by tracking the mobility of participating EVs and coordinating the hourly day-ahead solution at the sub-transmission level by sending the optimal signals to end users to manage charging/discharging of individual EVs.

The time step in the proposed optimization is one hour in which the dispatch of the entities is fixed during each time step. The intra-hour charging/discharging sequences can be addressed once the time step for the optimization problem is decreased to less than an hour. In the presumed sub-hourly scenario, the objective function and constraints would be modified accordingly to address the intra-hour generation schedule and dispatch of entities in the electricity market.

The objective in this paper is to minimize the power grid operation cost subject to the system, EV, and generation unit constraints (2)–(18). The objective function (1) consists of the generation cost of thermal units, startup and shutdown costs of thermal and hydro units, and the operation cost of EV fleets. The EV operation cost depends on the number of vehicles and charging/discharging depth and frequency [11]. The EV operation cost is considered as a convex function in this study, which is piecewise linearized and incorporated into the proposed MIP formulation.

The system and generating unit constraints are shown in (2)–(18). The generation-load balance constraint is shown in (2). Detailed thermal unit constraints are presented in [16]. Hydro unit constraints other than (3)–(5) are given in [17]. The water to power curve of hydro unit k is a nonlinear, non-convex curve [18], in which the hydro unit power generation has a nonlinear correlation with the water flow through

the turbine and the water head. Using auxiliary binary variables, the non-convex water to power curve can be converted into a piecewise linearized model and incorporated into the proposed MIP formulation [19], [20]. Equation (3) shows the piecewise linear mixed-integer formulation of non-convex water-to-power curve and (4), (5) represent the startup and shutdown costs of hydro units. The wind curtailment constraint is shown in (6) in which the wind generation forecast is equal to the wind generation dispatch plus any wind curtailments. The wind curtailment occurs when there is an insufficient ramping capability of thermal units or significant transmission congestion in the system to utilize the available wind energy. The EV fleet constraints are shown in (7)–(14). The net hourly energy drawn from/delivered to the grid and the dispatched power of EV fleet is given in (7). Equation (8) shows that the charging/discharging/idle modes of EV fleets are mutually exclusive. Equations (9), (10) represent charging/discharging power limits. The energy balance in EV batteries is represented by (11).

In addition, (12), (13) show the capacity limit in each fleet. The piecewise linear representation of the storage charging/discharging cost curve is shown in (14), which incorporates the storage depth of discharge and cycles to failure to represent the cost of energy withdrawn or delivered by EVs. The depth of discharge has a negative correlation with the cycles to failure in batteries [21]. With a higher depth in battery charging/discharging, the number of cycles to failure decreases which in turn will increase the cost of EV charging/discharging [11].

For NiMH batteries, it is shown that as the depth of discharge increases from 20% to 100% the cycles to failure decreases 10–15 times [21]. Considering a fixed cost for the battery, the charging/discharging cost representing the battery degradation is calculated according to [11] in which the cost increases as the depth of discharge increases. Hence, the operation cost of EV is correlated with the depth of discharge as shown in (14) which is the linearized representation of the quadratic function. The present price of a complete EV battery pack is 500–600 $/kWh which is reduced to 200 $/kWh and 160 $/kWh by 2020 and 2025 respectively [22]. In the consumer-controlled scheme, (15) sets the SOC of EV to a certain level (100% in this case) at certain operation hours. Equations (16)–(18) represent the dc power flow constraints.

The hourly scheduling problem in (1)–(18) is a large-scale, nonlinear, non-convex, non-deterministic polynomial-time hard (NP-hard) optimization problem [23].

$$Min \begin{array}{l} \sum_t \sum_i (F_{c,i}(P_{i,t}) + SU_{i,t} + SD_{i,t}) + \\ \sum_t \sum_k (SU_{k,t} + SD_{k,t}) + \sum_t \sum_v C_{v,t} \end{array} \tag{1}$$

s.t.

$$\sum_i P_{i,t} + \sum_v P_{v,t} + \sum_k P_{k,t} + \sum_w P_{w,t} = P_{D,t} \tag{2}$$

$$\begin{cases} P_{k,t} = P_k^{\min} I_{k,t} + \sum_m b_{m,k} q_{m,k,t} \\ q_{k,t} = q_k^{\min} I_{k,t} + \sum_m q_{m,k,t} \\ 0 \le q_{m,k,t} \le \left(q_{m,k}^{\max} - q_{m-1,k}^{\max}\right) \delta_{k,t}^{m-1} \quad \forall m \\ q_{m,k,t} \ge \left(q_{m,k}^{\max} - q_{m-1,k}^{\max}\right) \delta_{k,t}^{m} \quad \forall m \in [1, NM_k - 1] \end{cases} \tag{3}$$

$$SU_{k,t} \ge CS_k \cdot (I_{k,t} - I_{k,t-1}) \tag{4}$$

$$SD_{k,t} \ge CD_k \cdot (I_{k,t-1} - I_{k,t}) \tag{5}$$

$$P_{w,t} + P_{d,w,t} = P_{f,w,t} \tag{6}$$

$$\begin{cases} E_{v,t}^{net} = P_{dc,v,t} - \eta_v \cdot P_{c,v,t} \\ P_{v,t} = P_{dc,v,t} - P_{c,v,t} \end{cases} \tag{7}$$

$$I_{dc,v,t} + I_{c,v,t} + I_{i,v,t} = N_{v,t} \tag{8}$$

$$I_{c,v,t} \cdot P_{c,v}^{\min} \le P_{c,v,t} \le I_{c,v,t} \cdot P_{c,v}^{\max} \tag{9}$$

$$I_{dc,v,t} \cdot P_{dc,v}^{\min} \le P_{dc,v,t} \le I_{dc,v,t} \cdot P_{dc,v}^{\max} \tag{10}$$

$$E_{v,t} = E_{v,t-1} - E_{v,t}^{net} - (1 - N_{v,t}) \cdot DR_{v,t} \tag{11}$$

$$E_v^{\min} \le E_{v,t} \le E_v^{\max} \tag{12}$$

$$E_{v,0} = E_{v,NT} \tag{13}$$

$$\begin{cases} C_{v,t} = N_{v,t} \cdot \left(\sum_m b_{m,v} \cdot P_{m,v,t}\right) \\ 0 \le P_{m,v,t} \le P_{m,v}^{\max} \\ N_{v,t} \cdot |E_{v,t} - E_{v,t-1}| = \sum_m P_{m,v,t} \end{cases} \tag{14}$$

$$E_{v,\hat{T}} = E_v^{\max} \tag{15}$$

$$\begin{array}{l} \sum_{i \in B_b^i} P_{i,t} + \sum_{w \in B_b^w} P_{w,t} + \sum_{v \in B_{b,t}^v} P_{v,t} + \sum_{k \in B_b^k} P_{k,t} \\ = \sum_{d \in D_b} P_{D,t}^d + \sum_{l \in L_{f,b}} PL_{l,t} - \sum_{l \in L_{t,b}} PL_{l,t} \end{array} \tag{16}$$

$$PL_{l,t} = \frac{(\theta_{j,t} - \theta_{o,t})}{X_{j,o}} \tag{17}$$

$$|PL_{l,t}| \le PL_l^{\max} \tag{18}$$

Fig. 2 shows the flowchart in which the large-scale scheduling problem is decomposed into a master MIP problem, represented by (1)–(15), and an LP subproblem (19)–(24), (17), (18). The subproblem checks for possible network violations in the hourly commitment of generating units calculated in the master solution, which is subjected to the power balance at each bus (20) and line flow limits (17), (18). Benders cuts are generated according to the violations and imposed on the master problem solution. If the value of (19) is larger than the specified tolerance, the current master problem solution will violate transmission network constrains, and a feasibility cut (25) will be formed and added to the master problem for the solution of next iteration.

$$Min\ W_t(\hat{I}_t, \hat{P}_t) = \sum_b (MP_{1,t,b} + MP_{2,t,b}) \tag{19}$$

s.t.

$$\begin{array}{l} \sum_{i \in B_b^i} P_{i,t} + \sum_{w \in B_b^w} P_{w,t} + \sum_{v \in B_{b,t}^v} P_{v,t} + \sum_{k \in B_b^k} P_{k,t} + MP_{1,t,b} \\ \quad - MP_{2,t,b} = \sum_{d \in D_b} P_{D,t}^d + \sum_{l \in L_{f,b}} PL_{l,t} - \sum_{l \in L_{t,b}} PL_{l,t} \end{array}$$

$$MP_{1,t,b}, MP_{2,t,b} \ge 0 \tag{20}$$

$$P_{i,t} = \hat{P}_{i,t} \qquad \pi_{i,t} \tag{21}$$

$$P_{v,t} = \hat{P}_{v,t} \qquad \lambda_{v,t} \tag{22}$$

$$P_{k,t} = \hat{P}_{k,t} \qquad \rho_{k,t} \tag{23}$$

$$P_{w,t} = \hat{P}_{w,t} \qquad \mu_{w,t} \tag{24}$$

$$\begin{array}{l} W_t(I_t, P_t) = W_t(\hat{I}_t, \hat{P}_t) + \sum_i \pi_{i,t}(P_{i,t} - \hat{P}_{i,t}) \\ \quad + \sum_v \lambda_{v,t}(P_{v,t} - \hat{P}_{v,t}) + \sum_k \rho_{k,t}(P_{k,t} - \hat{P}_{k,t}) \\ \quad + \sum_w \mu_{w,t}(P_{w,t} - \hat{P}_{w,t}) \le 0 \end{array} \tag{25}$$

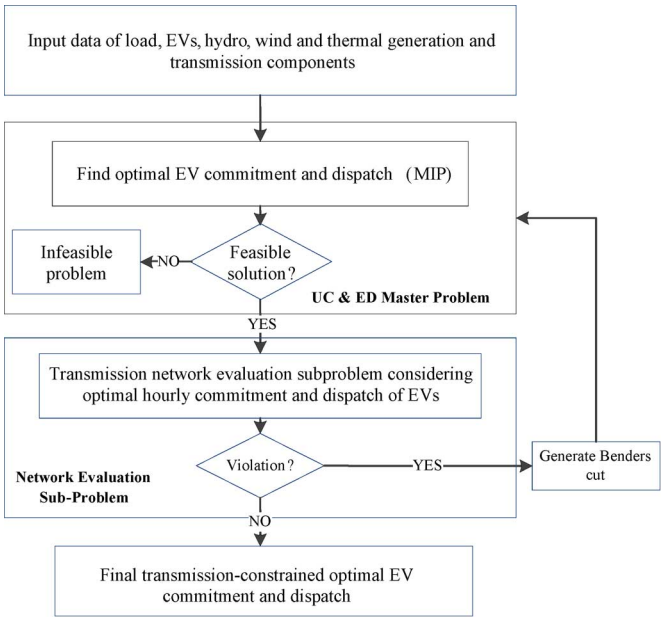

Fig. 2. Network-constrained hourly generation scheduling with the integration of aggregated EV.

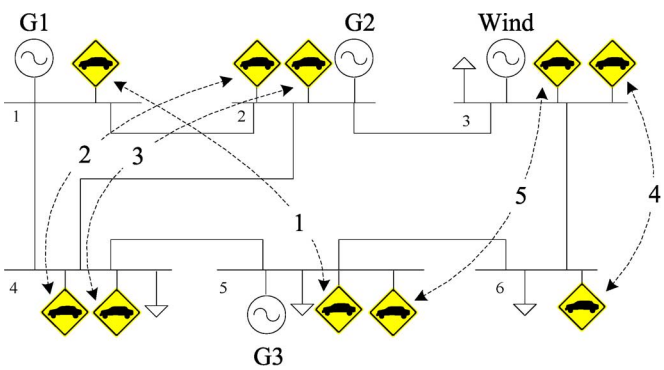

Fig. 3. 6-bus power grid.

TABLE I
THERMAL UNIT CHARACTERISTICS

Unit	a ($/MW^2)	b ($/MW)	c ($/h)	P_{min} (MW)	P_{max} (MW)	SU ($)	SD ($)	Min. Up (h)	Min Dn. (h)
G1	0.099	6.589	211.4	100	320	100	50	4	3
G2	0.203	7.629	217.4	10	160	200	40	3	2
G3	0.494	10.07	102.8	10	100	80	10	1	1

TABLE II
TRANSMISSION LINE CHARACTERISTICS

Line ID	From Bus	To Bus	Impedance (p.u)	Max Power Flow (MW)
1	1	2	0.170	65
2	1	4	0.258	70
3	2	4	0.197	40
4	5	6	0.140	40
5	3	6	0.018	75
6	2	3	0.037	80
7	4	5	0.037	65

TABLE III
EV FLEET CHARACTERISTICS

EV fleet No.	Min Cap. (MWh)	Max Cap. (MWh)	Min Charge/ Discharge (kW)	Max Charge/ Discharge (MW)	a ($/MW^2)	b ($/MW)	c ($/h)
1	13.152	65.76	7.3/6.2	24.8/21.08	0.17	8.21	0
2	10.96	54.8	7.3/6.2	14.58/12.4	0.20	8.21	0
3	5.48	27.4	7.3/6.2	7.29/6.2	0.41	8.21	0
4	8.768	43.84	7.3/6.2	11.67/9.92	0.25	8.21	0
5	10.96	54.8	7.3/6.2	14.58/12.4	0.20	8.21	0

TABLE IV
EV FLEET TRAVEL CHARACTERISTICS

EV fleet No.	Number of EVs	First Trip				Second Trip			
		Departure		Arrival		Departure		Arrival	
		Time	Bus	Time	Bus	Time	Bus	Time	Bus
1	3,400	6:00	5	8:00	1	17:00	1	19:00	5
2	2,000	7:00	4	8:00	2	16:00	2	17:00	4
3	1,000	5:00	4	7:00	2	16:00	2	18:00	4
4	1,600	5:00	6	6:00	3	17:00	3	18:00	6
5	2,000	7:00	5	9:00	3	18:00	3	20:00	5

III. CASE STUDIES

In this section, a 6-bus and the modified IEEE 118-bus power grids are studied to demonstrate the impact of V2G on the grid operation cost, hourly locational marginal prices (LMPs), hourly wind curtailment, and optimal commitment and dispatch of thermal, hydro and wind units.

A. 6-Bus Power Grid

A 6-bus power system shown in Fig. 3 is considered to evaluate the impact of integrating and operating EVs. The generation and transmission line data are shown in Tables I and II, respectively. Tables III and IV show the five EV categories, which are based on driving patterns, i.e., departure and arrival times, and driving energy requirements. The aggregated max/min capacity, charging/discharging patterns, and the available energy for each fleet are given. It is assumed that EVs are connected to the grid through level II charging stations. The residential and commercial level II charging station has 3.8–7.2 kW and 7.2–16.8 kW power capacity respectively [15]. Here the charging/discharging power capacity for each EV is considered as 7.3 and 6.2 kW, respectively. The battery capacity for each EV in the first fleet is 19 kWh and the battery capacity of each EV in the second through the fifth fleet is 27.4 kWh. Considering that the price of the battery is forecasted to decrease by 2020, the battery cost is considered as 200 $/kWh in this case [22].

The ratio of stored energy in the battery to the energy drawn from the grid is 88%, considering the battery and rectifier efficiency [24]. The cycle efficiency is 83.6% for a charging/discharging efficiency of 95% [25]. Here the EV cycle efficiency for charging/discharging is 85%, which represents the ratio of the energy stored in batteries to the energy drawn from the grid. The estimated driving distance by an EV is 12 000 miles per year, which is 32.88 miles per day on average [26], [27]. Assuming that the EV can run 3.65 miles/kWh [11], the average energy required for driving an EV is 9 kWh/day. Hence, the hourly energy required by individual fleets are 7.65, 9.00, 2.25, 7.20, and 4.50 MWh, respectively. For simplicity, we assume the energy required for driving in one direction is the same as that of returning to the same place. The installed wind capacity is 75 MW, which is 30% of the system peak load. The total available wind generation is 11% of the total system demand. In the grid-controlled scheme, power grid operators will optimize charging/discharging decisions for EVs based on

TABLE V
HOURLY COMMITMENT OF GENERATION UNITS IN CASE 1

Unit	Hours (1-24)																							
G1	1	1	1	1	1	1	1	1	1	1	1	1	1	1	1	1	1	1	1	1	1	1	1	1
G2	1	1	1	1	1	1	1	1	1	1	1	1	1	1	1	1	1	1	1	1	1	1	1	1
G3	0	0	1	1	1	1	1	1	1	1	1	1	1	1	1	1	1	1	1	1	1	1	1	1

TABLE VI
HOURLY POWER DISPATCH OF EVS IN CASE 1 (MW)

Fleet	Hours (1-12)											
1	-5.49	0	0	0	0	0	0	-1.72	0	0	0	0
2	0	0	0	0	0	-4.53	0	0	0	0	0	0
3	0	0	0	0	0	0	-6.45	0	0	0	0	0
4	0	0	0	0	0	-8.97	-6.49	0	0	0	0	0
5	0	0	0	0	0	-6.23	0	0	0	0	0	0
Fleet	**Hours (13-24)**											
1	-0.81	0	0	-15.47	0	0	-7.37	-5.13	0	0	0	0
2	-12.9	0	0	0	0	0	0	0	0	0	-3.75	0
3	-4.14	0	0	0	0	0	0	0	0	0	0	0
4	-1.48	0	0	0	0	0	0	0	0	0	0	0
5	-14.6	-0.35	0	0	0	0	0	0	0	0	0	0

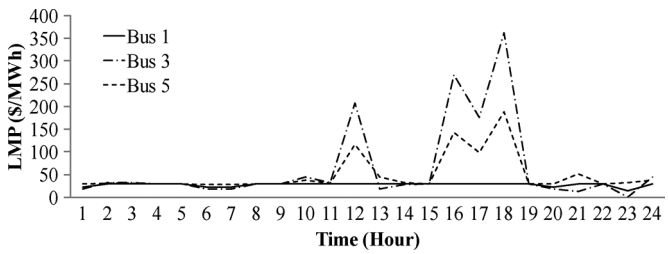

Fig. 4. Bus LMPs in Case 1.

prevailing conditions. In contrasts, hourly SOCs in the consumer-controlled scheme represent charging/discharging states of EVs that are required by consumers.

The following four cases are presented in this study:

Case 1) EVs do not perform V2G in the grid-controlled scheme.

Case 2) EVs do not perform V2G in the consumer-controlled scheme.

Case 3) EVs perform V2G in the grid-controlled scheme.

Case 4) EVs perform V2G in the consumer-controlled scheme.

These cases are studied as follows:

Case 1: EVs Do Not Perform V2G in the Grid-Controlled Scheme: In this case, EVs are modeled as a distributed demand and the optimal hourly schedule for EVs is calculated according to driving patterns and power grid operation requirements. The hourly forecasts for load, wind generation, and driving requirements are available.

The grid operation cost in Case 1 is $121 396.10 and the wind curtailment is 1.52 MWh. Table V shows the hourly commitment of thermal generators in which the most expensive unit, G3, is committed for 22 hours for managing the transmission congestion. Table VI shows the dispatch of EV fleets in which the negative numbers indicate the energy drawn from the grid (i.e., no V2G is considered). Fig. 4 shows the LMPs at buses 1, 3, and 5. In this case, EVs are charged when hourly LMPs are low.

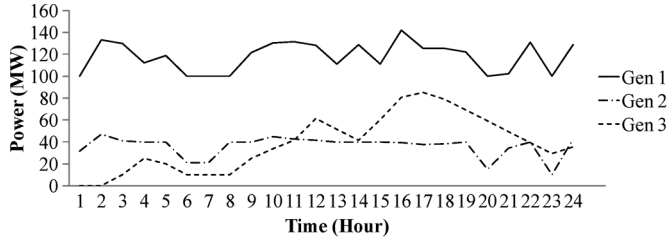

Fig. 5. Hourly generation dispatch in Case 1.

The energy for driving EV fleets is drawn from the grid and stored at low LMP hours. Table VI shows that as the LMPs at buses 3 and 5 are higher at hours 12:00 and 16:00–18:00, the corresponding EVs will not be charged. The highlighted hours in Table VI are the hours when the EV fleets 4 and 5 are connected to buses 3 but not charged. Table VI also shows the energy required by the first EV fleet, for traveling from bus 5 to bus 1 at hours 6:00 and 7:00, is provided at hour 1:00 when the LMP at bus 5 is low (30 $/MWh). Although the LMP at hours 6:00 and 7:00 is lower (i.e., 27.984 $/MWh), the EV fleet has already departed bus 5. Once located at bus 1, the EV energy required for returning to bus 5 is drawn at hours 8:00, 13:00, and 16:00 in which the LMP is 30 $/MWh. After returning to bus 5 at hour 19:00, the EV fleet will be partially charged at hours 19:00 and 20:00 when the energy price is low (30 $/MWh), and again at hour 1:00 of the next day. Hence the energy is drawn by EV fleets when and where the electricity price is low.

The thermal generation portfolio is variable when serving the hourly system and EV fleet demand. Fig. 5 shows the hourly generation dispatch in which the G3's dispatch demonstrates a high variability as it exceeds 80 MW at peak hours.

The EV mobility will support the hourly operation of power grid. If the EV fleets are assumed to be stationary at a bus, the grid operation cost will increase to $122 168.34 and the wind curtailment will increase to 11.149 MWh. Thus, the mobility of EV can reduce the grid operation cost and the wind curtailment.

Case 2: EVs Do Not Perform V2G in the Consumer-Controlled Scheme: In this case, the SOC is set to 100% when the EV fleet departs a bus. The power grid operation cost is $121 585.52 and the wind curtailment is 1.40 MWh. The hourly unit commitment is the same as those in Table V. However, Table VII shows a different power dispatch for supplying EVs. By comparison, the consumer-controlled mode imposes further constraints on the EV charging/discharging which will lead to higher grid operation costs. Here, the wind curtailment is decreased by 0.12 MWh (i.e., 1.52 − 1.4) which demonstrates a lack of correlation between wind curtailments and the grid operation costs, as we optimize the hourly grid operation over a multi-hour time horizon.

The power grid operation cost is higher when consumers manage the EV charging/discharging periods; however, the individual EV energy payment may not increase. The hourly energy payment by each fleet is procured by hourly LMPs multiplied by the EV energy requirement. For instance, for the fourth fleet, the energy drawn at hours 0:00–4:00, 6:00–16:00, and 18:00–24:00 in the grid-controlled scheme (Case 1) are 0, 16.94, and 0 MWh, respectively, and the energy payments are $0, $309.713, and $0. By comparison, the consumer-controlled scheme (Case 2) shows the energy drawn are 0.01, 8.47, and 8.46 MWh and energy payments are $0.3, $110.91, and $253.92, respectively. Thus, the total energy payments in Cases

TABLE VII
HOURLY POWER DISPATCH OF EVS IN CASE 2 (MW)

Fleet	Hours (1-12)											
1	-0.01	0	0	-11.85	0	0	0	-1.72	-15.5	0	0	0
2	-0.58	0	0	0	0	-10.0	0	0	0	0	0	0
3	-0.01	0	0	0	0	0	-5.29	0	0	0	0	0
4	0	0	0	-0.01	0	0	0	0	0	0	0	0
5	-5.03	0	0	-0.01	0	-0.01	0	0	0	0	0	0
Fleet	Hours (13-24)											
1	0	0	-0.01	-0.80	0	0	-6.142	0	0	0	0	0
2	-10.6	0	0	0	0	0	0	0	0	0	0	0
3	-0.01	0	0	0	0	0	0	-0.84	0	0	-4.45	0
4	-8.47	0	0	0	0	0	-8.464	0	0	0	0	0
5	-10.6	0	0	0	0	0	0	-4.47	0	-1.07	0	0

TABLE VIII
HOURLY COMMITMENT IN CASE 3

Unit	Hours (1-24)																							
G1	1	1	1	1	1	1	1	1	1	1	1	1	1	1	1	1	1	1	1	1	1	1	1	1
G2	1	1	1	1	1	1	1	1	1	1	1	1	1	1	1	1	1	1	1	1	1	1	1	1
G3	0	0	0	0	0	0	1	1	1	1	1	1	1	1	1	1	1	1	1	1	1	1	1	1

1 and 2 are \$309.713 and \$365.04, respectively, with a higher EV energy payment for the fourth fleet in Case 2. In the consumer-controlled scheme (Case 2), the fourth fleet is charged at bus 6, which increases the energy payment. However, the conclusion may not apply to all fleets. For instance, the energy payment of the second fleet in the grid-controlled scheme is \$514.982 as compared to \$506.622 in the consumer-controlled scheme.

The total energy payments in the grid-controlled and consumer-controlled schemes are \$2580.225 and \$2661.273, respectively, which shows a lower payment in the grid-controlled case. The generation profile in the consumer-controlled scheme is similar to that in Fig. 5. Once again, if EV fleets are stationary, the grid operation cost and the wind curtailment will increase to \$122 200.91 and 11.35 MWh, respectively, which emphasize the effect of EV mobility on the optimization of power grid operation.

Case 3: EVs Perform V2G in the Grid-Controlled Scheme: V2G could decrease the power grid operation cost by reducing the hourly wind curtailment and shortening the hourly commitment of expensive units. Compared to Case 1, the grid operation cost and the wind curtailment, are reduced to \$115 541.36 and 0 MWh, respectively. Table VIII shows the hourly unit commitment of thermal units. In comparison with Case 1, the commitment of G3 is decreased by 4 hours.

Using V2G the fleets are discharged to the grid where and when the electricity price is high and draw energy from the grid where and when the electricity price is low. In Table IX, the first EV fleet, which travels between buses 5 and 1, will deliver the power back to the grid (V2G) at hour 5:00 when the LMP at bus 5 is high (53.294 \$/MWh). The EV fleet at bus 5 will not be charged at hours 19:00 to the 5:00 am of the next day, because the LMPs are high (33.693–52.294 \$/MWh). The fleet will be charged at bus 1 when the LMP is low (30 \$/MWh). Also, the fifth EV fleet which travels between buses 5 and 3 will not be

TABLE IX
POWER DISPATCH OF EVS IN CASE 3 (MW)

Fleet	Hours (1-12)											
1	0	0	0	0	0.725	0	0	-5.9	0	-15.5	0	0
2	-7.0	0	0	0	0	-0.47	0	-12.9	0	0	0	0
3	0	0	0	0	0	0	-7.29	-3.29	0	0	0	0
4	0	-0.99	1.96	-0.96	0	-11.6	-11.6	-10.3	0	0	0	5.49
5	0	0	0	0	0	0	0	0	-11.2	0	0	0
Fleet	Hours (13-24)											
1	-15.5	0	0	0	0	0	0	0	0	0	0	0
2	-13	-7.98	0	0	12.4	7.50	0	0	0	0	-3.25	0
3	-6.45	0	0	0	0	5.48	0	0	0	0	0	0
4	-11.6	0	-2.39	3.86	0	9.92	-0.08	2.14	3.57	-1.71	2.40	0
5	-14.6	-11.8	-10.9	10.9	12.4	0	0	0	0	0	0	0

charged/discharged at bus 5 since the min/max LMPs are 24.472 and 60.474 \$/MWh, respectively, which occur at bus 3. Hence, it is more economical to charge at the lowest LMP located at bus 3 and discharge at the highest LMP located at the same bus.

The EV mobility once again will reduce the power grid operation costs. If EVs are stationary, the power grid operation cost and the wind curtailment are increased to \$117 424.15 and 1.196 MWh, respectively. The required driving energy, maximum storage capacity, and SOC constraints may limit the contribution of EV mobility to the power grid operation. EVs can reduce the power grid operation cost by V2G as they transfer energy from low LMP buses to high LMP buses. In this case, the fourth fleet, which travels between buses 6 and 3, will leave bus 6 in the morning with a SOC of 36.4% and return in the evening with a SOC of 74.8%. Here, energy is transferred from bus 3 to bus 6 through mobility.

EVs can also reduce the grid operation cost even if they will not transfer energy between buses. The SOC of the fifth fleet, which travels between buses 5 and 3, is 36.4% when leaving bus 5 or returning to bus 5. The power exchange is possible when the fleet is connected to bus 3, where the max/min LMPs occur when the EV is connected. Hence, no energy is transferred in this case from bus 5 to bus 3 or vice versa. Moreover, consumer constraints on SOC can limit the EV energy transfer between buses.

The V2G option for the generation scheduling will not only decrease the grid operation cost but also reduce the generation variability in the power grid. Comparing Figs. 5 and 7, it is shown that the generation profile is less variable in Case 3. The standard deviation of the total generation in Cases 1 and 3 are 37.55 and 34.57 MW, respectively. Hence, a more flexible EV control mode can help mitigate the variability of generation dispatch when they try to cope with a large integration of variable renewable resources.

Case 4: EVs Perform V2G in the Consumer-Controlled Scheme: In this case, the consumers set the SOC of EVs to 100% when departing a bus. The constraints imposed by the consumers will increase the operation cost of the power grid. Compared to Case 3, the grid operation cost is increased to \$119 084.33 while the wind curtailment is 0 MWh. Table X shows that G3 is committed hourly in the consumer-controlled scheme as compared with Case 2; however, the grid operation cost is lowered. The wind curtailment is also decreased to 0

TABLE X
HOURLY COMMITMENT OF UNITS IN CASE 4

Unit	Hours (1-24)																							
G1	1	1	1	1	1	1	1	1	1	1	1	1	1	1	1	1	1	1	1	1	1	1	1	1
G2	1	1	1	1	1	1	1	1	1	1	1	1	1	1	1	1	1	1	1	1	1	1	1	1
G3	1	1	1	1	1	1	1	1	1	1	1	1	1	1	1	1	1	1	1	1	1	1	1	1

TABLE XI
HOURLY POWER DISPATCH OF EVS IN CASE 4 (MW)

Fleet	Hours (1-12)											
1	-15.5	0	0	0	-2.53	0	0	-1.72	0	0	0	0
2	-12.3	0	0	0	0	-12.9	0	0	0	0	0	0
3	-2.04	0	0	0	0	0	-5.29	0	0	0	0	0
4	0	-10.3	-4.33	-10.3	0	-8.47	0	0	0	1.93	0.01	5.49
5	0	0	0	0	0	-10.6	0	0	0	1.96	0.01	0
Fleet	Hours (13-24)											
1	0	0	-15.5	-0.81	0	0	0	0	0	0	0	0
2	-10.6	0	0	0	12.4	0	0	0	0	0	0	0
3	0	0	0	0	0	0	0	0	0	0	-3.25	0
4	-8.73	0	0	0	0	6.68	-2.93	2.14	5.282	0	2.403	0
5	-12.9	0	0	0	0	0	0	0	0	0	0	0

TABLE XII
MAXIMUM LMPS IN CASES 1–4 ($/MWh)

Bus	Grid-Controlled Scheme		Consumer-Controlled Scheme	
	Case 1	Case 3	Case 2	Case 4
1	30.0	30.0	30.0	30.0
2	32.0	32.0	32.0	32.0
3	361.9	121.6	361.9	336.0
4	147.3	64.1	147.3	137.9
5	188.0	75.0	188.0	175.5
6	342.1	116.3	342.1	317.7

MW as compared to Case 2. Once again, it is shown that V2G can reduce the power grid operation cost and wind curtailments.

If the EV is stationary, the grid operation cost and the wind curtailment will be $119 796.84 and 1.55 MWh, respectively. In the consumer-controlled schemes, the SOC of the fleet is always set at 100% when leaving a bus, which eliminates the ability to transfer energy between buses. Fig. 8 shows that, as we impose consumer constraints, the generation dispatch is not as smooth as that in Case 3.

Table XI shows the EV fleet dispatch. The negative and positive numbers in the table represent charging and discharging of the fleet storage respectively. In Table XI, the second fleet will set its SOC to 100% at hour 16 by charging at hour 13. Table XII shows the maximum LMPs in four cases. Here, V2G can reduce the power grid congestion in grid-controlled schemes; however, V2G may not be as effective in consumer-controlled schemes. The comparisons of Cases 3 and 1 and Cases 4 and 2 show that V2G will lead to a lower congestion in the grid-controlled scheme. V2G can reduce the maximum LMPs by reducing the transmission congestion. Figs. 5–6 show that the maximum LMP is lower in Case 3 as compared to that in Case 1.

B. 118-Bus Power Grid

The modified IEEE 118-bus system shown in http://motor.ece.iit.edu/EV/118.emf is used to evaluate the impact of EV operation on the power grid optimization. Five 150 MW wind generation sites are considered at buses 12, 31, 66, 72, and 100,

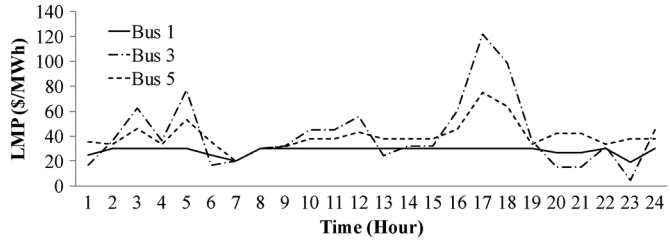

Fig. 6. LMPs in grid-controlled scheme in Case 3.

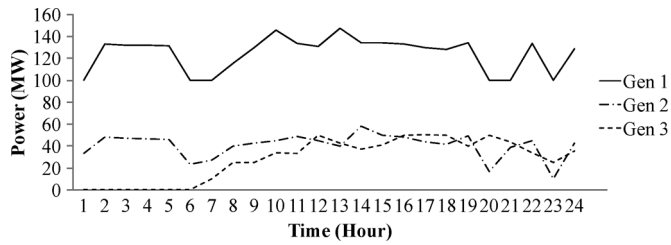

Fig. 7. Hourly generation dispatch in Case 3.

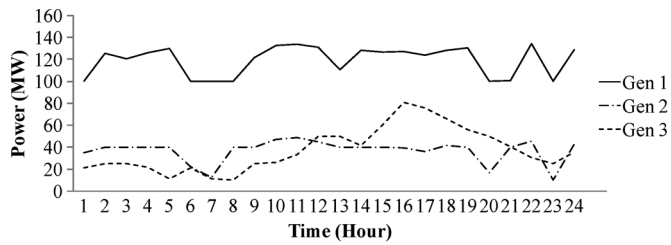

Fig. 8. Hourly generation dispatch in Case 4.

TABLE XIII
WIND SPEED PROFILE IN DIFFERENT SITES

	site 1	site 2	site 3	site 4	site 5
Weibull Coefficient	1.17	2.03	2.19	2.9	2.26
Auto Correlation Factor	0.761	0.943	0.957	0.88	0.928
Diurnal Wind Pattern	0.11	0.0944	0.0969	0.0196	0.0668
Hour of Peak Wind Speed	24	14	13	20	22

respectively. Table XIII shows the wind speed information on the proposed five wind sites. One hundred thousand EVs are divided into 5 fleets which are based on their driving patterns, in which the number of EVs are 34 000, 20 000, 10 000, 16 000, and 20 000, respectively. Table XIV shows the EV fleet characteristics. The EV battery cost is 600 $/kWh. The same four cases discussed in Example A are considered here. Table XV shows the grid operation cost and the wind curtailment for all four cases. Here, the grid-controlled scheme will lead to a lower grid operation cost, which is due to fewer imposed constraints. Moreover, V2G can reduce the operation cost of the power grid in both grid-controlled and consumer-controlled schemes. Table XV shows that the application of V2G in the grid-controlled scheme may further reduce the grid operation cost.

The comparison of Cases 2 and 4 shows that the application of V2G in consumer-controlled scheme may increase the wind curtailment while decreasing the operation cost of power grid. Hence, there may be no apparent correlation between the wind curtailment and the operation cost of power grid.

The power grid operation cost will be decreased as the EV storage capacity is increased. In Fig. 9, the operation cost factor (OCF) shows the charging/discharging cost as a percentage of nominal cost of storage operation. Here, the grid operation cost

TABLE XIV
EV FLEET CHARACTERISTICS

EV Fleet	Min Energy (MWh)	Max Energy (MWh)	Charge/Discharge Min (KW)	Charge/Discharge Max (MW)	a ($/MW^2)	b ($/MW)	c ($/h)
1	131.52	986.4	7.3/6.2	248/210.8	0.57	27.35	0
2	109.6	822	7.3/6.2	145.8/124	0.68	27.35	0
3	54.8	411	7.3/6.2	72.9/62	1.36	27.35	0
4	87.68	657.6	7.3/6.2	116.7/99.2	0.85	27.35	0
5	109.6	822	7.3/6.2	145.8/124	0.68	27.35	0

TABLE XV
FINAL RESULTS FOR ALL FOUR CASES

Case	Cost ($)	Wind Curtailment (MWh)
1	1,983,586	1,621
2	1,995,336	1,620
3	1,974,030	1,614
4	1,992,155	1,642

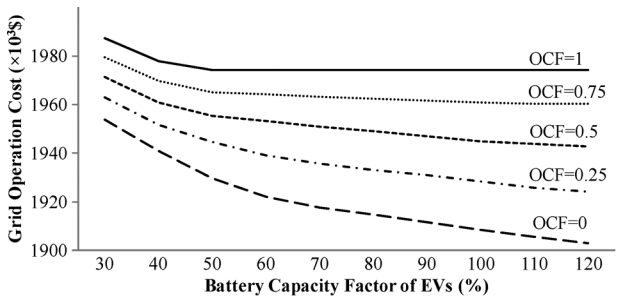

Fig. 9. Grid operation costs with different OCFs in grid-controlled scheme.

drops at lower OCFs. In addition, a higher storage capacity of EVs will decrease the grid operation cost.

In the consumer-controlled scheme, a larger storage capacity may not always reduce the power grid operation cost as the imposed SOC constraints would limit the EV contribution to affect the operation cost of the system. A higher charging/discharging cost will restrict the EV's participation in V2G as operation costs will be higher. Since EVs are considered as new types of demands in the system, the integration of EV fleets will increase the operation cost. However, the comparison of V2G and non-V2G case and the mobile with stationary EV fleets show that the integration of mobile EV fleets with V2G would reduce the system operation cost and increase the penetration level of renewable energy by reducing the wind curtailment. Since the cost of charging/discharging is high, the application of V2G would be most effective in a congested power system with higher electricity prices. Once the power system is not congested, it may be more economical to commit less expensive generation units for supplying hourly loads.

IV. DISCUSSIONS

EVs represent distributed and mobile demands in power grids. The mobility of EV can impose additional constraints for supplying local loads. The EV operation can reduce the impact of renewable generation intermittency in power grids.

In this paper, two operation states are considered for EVs. The first state considers EVs as distributed loads, which can only draw energy from the grid. The second state allows EVs to perform V2G in the power grid. In each state, two operation schemes are proposed. In the grid-controlled scheme, the ISO will operate the power grid while satisfying the energy requirements for driving fleets. In the consumer-controlled scheme, consumers will set the charging/discharging criteria for EVs which are fully charged before they leave a bus.

It is shown that V2G can reduce the grid operation cost and alleviate the transmission congestion by drawing energy at one time and location and delivering it to another time and location. When consumers set the SOC at certain time periods, the grid operation cost will increase as further constraints are imposed. Setting the SOC level will restrict the EVs' ability to transfer energy among critical power system locations when required.

The mobility of EVs will facilitate the energy transfer without facing transmission constraints. EVs can optimize the energy transfer from one location in power systems to another for alleviating the transmission congestion and decreasing the grid operation costs.

EVs can act as distributed storage even if they are not transferring energy through the network, which can increase and enhance the penetration level of renewable sources. Also, the variability of thermal generation will be reduced once EVs can store and deliver energy to the congested grid.

The utilization of aggregated EVs in power grids may introduce additional barriers. The major impediment is the charging/discharging costs of EVs. Also, the frequent charging and discharging sequences could reduce the battery life, which would impose further limitations on the operating schedule of EVs as storage and load. However, the charging/discharging costs of EVs are deemed more reasonable once we consider the alternate cost of transmission congestion and increases in bus LMPs.

EVs are mobile and distributed loads which can offer storage at certain buses. This feature will make them different from conventional storage technologies such as compressed air and pumped storage (PS), which are mainly designed to store and deliver energy in the power grid. The EV storage is not primarily designed to be utilized as the grid storage, and EV requirements for mobility between locations could impose further restrictions in power systems for utilizing EVs as storage facilities.

V. CONCLUSIONS

In this paper, the impact of EV operation modes on power grid operations is evaluated. The proposed model incorporates driving patterns, energy required for mobility and consumer behaviors, to procure the optimal charging/discharging schedule of EV fleets.

The contributions of the paper include:

- The modeling of hourly fleet constraints for procuring the optimal hourly charging/discharging decisions.
- The integration of transmission system constraints in the hourly operation of EV fleets.
- The modeling of wind energy variability in procuring the EV mobility decisions.
- The analysis of the impact of EV mobility and V2G on the hourly generation schedule of conventional units.

It is shown that V2G will reduce the grid operation cost and congestion in the power grid. The EV mobility can efficiently transfer energy in the power grid in proper times and locations. Once renewable energy resources are integrated, EVs can help reduce the generation dispatch variability and power grid operation costs by providing energy storage capabilities. However, the storage charging/discharging cost, limitations on storage capacity, the required energy for driving, and the consumer behavior will impose further restrictions on EV contributions to the optimal operation of power grids.

REFERENCES

[1] "Reducing greenhouse gas emissions from U.S. transportation" [Online]. Available: http://www.c2es.org/docUploads/ustransp.pdf

[2] "Technology roadmap electric and plug-in hybrid electric vehicles," International Energy Agency, Jun. 2011 [Online]. Available: http://www.iea.org/papers/2011/EV_PHEV_Roadmap.pdf

[3] S. S. Raghavan and A. Khaligh, "Electrification potential factor: Energy-based value proposition analysis of plug-in hybrid electric vehicles," *IEEE Trans. Veh. Technol.*, vol. 61, no. 3, pp. 1052–1059, Mar. 2012.

[4] "Global wind 2008 report," Global Wind Energy Council (GWEC) [Online]. Available: http://www.gwec.net/fileadmin/documents/Global%20Wind%202008%20Report.pdf

[5] S. Srinivasaraghavanand and A. Khaligh, "Time management," *IEEE Power Energy Mag.*, vol. 9, no. 4, pp. 46–53, Jul. 2011.

[6] M. Lu, C. Chang, W. Lee, and L. Wang, "Combining the wind power generation system with energy storage equipment," *IEEE Trans. Ind. Appl.*, vol. 45, no. 6, pp. 2109–2115, Nov. 2009.

[7] K. Clement, E. Haesen, and J. Driesen, "Coordinated charging of multiple plug-in hybrid electric vehicles in residential distribution grids," in *Proc. IEEE/PES PSCE'09*, pp. 1–7.

[8] E. Sortomme, M. M. Hindi, S. D. J. MacPherson, and S. S. Venkata, "Coordinated charging of plug-in hybrid electric vehicles to minimize distribution system losses," *IEEE Trans. Smart Grid*, vol. 2, no. 1, pp. 198–205, 2011.

[9] M. D. Galus and G. Andersson, "Integration of plug-in hybrid electric vehicles into energy networks," in *Proc. IEEE PowerTech 2009*, Bucharest, Romania, pp. 1–8.

[10] J. Wang, C. Liu, D. Ton, Y. Zhou, J. Kim, and A. Vyas, "Impact of plug-in hybrid electric vehicles on power systems with demand response and wind power," *Energy Policy*, vol. 39, pp. 4016–4021, Mar. 2011.

[11] J. Tomić and W. Kempton, "Using fleets of electric-drive vehicles for grid support," *J. Power Sources*, vol. 168, no. 2, pp. 459–468, Jun. 2007.

[12] Z. Peng, Q. Kejun, Z. Chengke, B. G. Stewart, and D. M. Hepburn, "A methodology for optimization of power systems demand due to electric vehicle charging load," *IEEE Trans. Power Syst.*, vol. 27, no. 3, pp. 1628–1636, 2012.

[13] EATON Residential Smart Charging Solution [Online]. Available: http://www.eaton.com

[14] M. E. Khodayar, L. Wu, and M. Shahidehpour, "Hourly coordination of electric vehicle operation and volatile wind power generation in SCUC," *IEEE Trans. Smart Grid*, 2012, accepted for publication.

[15] J. F. Manwell, J. G. McGowan, and A. L. Rogers, *Wind Energy Explained*. New York: Wiley, 2002.

[16] L. Wu, M. Shahidehpour, and T. Li, "Stochastic-security-constrained unit commitment," *IEEE Trans. Power Syst.*, vol. 22, no. 2, pp. 800–811, May 2007.

[17] T. Li and M. Shahidehpour, "Price-based unit commitment: A case of Lagrangian relaxation versus mixed integer programming," *IEEE Trans. Power Syst.*, vol. 20, no. 4, pp. 2015–2025, Nov. 2005.

[18] S. Mariano, M. Calado, and L. Ferreira, "Dispatch of head dependent hydro units: Modeling of optimal generation in electricity market," in *IEEE Power Tech*, Bucharest, Romania, Jun. 2009.

[19] S. Bisanovic, M. Hajro, and M. Dlakic, "Hydrothermal self-scheduling problem in a day-ahead electricity market," *Elect. Power Syst. Res.*, vol. 78, no. 9, pp. 1579–1596, Sep. 2008.

[20] L. Wu, M. Shahidehpour, and Z. Li, "GENCO's risk-constrained hydrothermal scheduling," *IEEE Trans. Power Syst.*, vol. 23, no. 4, pp. 1847–1858, Nov. 2008.

[21] "Advanced batteries for electric-drive vehicles a technology and cost-effectiveness assessment for battery electric vehicles, power assist hybrid electric vehicles, and plug-in hybrid electric vehicles," EPRI Tech. Rep., May 2004.

[22] R. Hensley, J. Newman, and M. Rogers, "Battery technology charged ahead," *Sustainability & Resource Productivity Practice, McKinsey Quarterly* Jul. 2012 [Online]. Available: http://www.mckinseyquarterly.com/Battery_technology_charges_ahead_2997

[23] X. Guan, Q. Zhai, and A. Papalexopoulos, "Optimization based methods for unit commitment: Lagrangian relaxation versus general mixed integer programming," *Proc. IEEE Power Eng. Soc. Meet.*, vol. 2, Jul. 2003.

[24] EPRI, "Environmental assessment of plug-in hybrid electric vehicles, volume 1: Nationwide greenhouse gas emissions," Jul. 2007 [Online]. Available: http://mydocs.epri.com/docs/CorporateDocuments/SectorPages/Portfolio/PDM/PHEV-ExecSum-vol1.pdf

[25] M. Stadler, C. Marnay, M. Kloess, G. Cardoso, G. Mendes, A. Siddiqui, R. Sharma, O. Mégel, and J. Lai, "Optimal planning and operation of smart grids with electric vehicle interconnection," *J. Energy Eng.*, vol. 138, no. 2, pp. 95–108, Feb. 2012.

[26] A. Saber and G. Venayagamoorthy, "Plug-in vehicles and renewable energy sources for cost and emission reduction," *IEEE Trans. Ind. Electron.*, vol. 58, no. 4, pp. 1229–1238, Apr. 2011.

[27] C. Roe, A. P. Meliopoulos, J. Meisel, and T. Overbye, "Power system level impacts of plug-in hybrid electric vehicles using simulation data," in *Proc . IEEE Energy*, Atlanta, GA, USA, Nov. 17–18, 2008.

Mohammad E. Khodayar (S'09–M'13) received the B.S. degree in electrical engineering from Amirkabir University of Technology (Tehran Polytechnic), Iran, the M.S. degree in electrical engineering from the Sharif University of Technology, Iran, and the Ph.D. degree in electrical engineering from the Illinois Institute of Technology, Chicago, in 2012.

He is presently a Senior Research Associate in the Robert W. Galvin Center for Electricity Innovation at the Illinois Institute of Technology. His research interests include renewable energies, electricity markets, and power system operation and control.

Lei Wu (M'07) received the B.S. degree in electrical engineering and the M.S. degree in systems engineering from Xi'an Jiaotong University, China, in 2001 and 2004, respectively, and the Ph.D. degree in EE from Illinois Institute of Technology, Chicago, in 2008.

He was a Senior Research Associate in the Robert W. Galvin Center for Electricity Innovation at Illinois Institute of Technology from 2008 to 2010. Presently, he is an Assistant Professor in the ECE Department at Clarkson University. His research interests include power systems restructuring and reliability.

Zuyi Li (SM'09) received the B.S. degree in EE from Shanghai Jiaotong University in 1995, the M.S. degree in EE from Tsinghua University, China, in 1998, and the Ph.D. degree in EE from Illinois Institute of Technology, Chicago, in 2002.

Presently, he is an Associate Professor in the Electrical and Computer Engineering Department at the Illinois Institute of Technology. His research interests include electricity market design and operation, renewable energy integration, and microgrid design and operation.

Prof. Li is the Associate Director of the Robert W. Galvin Center for Electricity Innovation at IIT.